別紙1

厚生労働科学研究費補助金

創薬基盤推進研究事業

肺癌における抗癌剤抵抗性を誘発する因子の阻害剤
探索のためのバイオ計測系の開発

平成24年度　総括・分担研究報告書

研究代表者　太田　力

平成 25（2013）年　5 月

別紙2

目　　次

別紙３

<div align="center">

厚生労働科学研究費補助金（創薬基盤推進研究事業）
総括・分担研究報告書

肺癌における抗癌剤抵抗性を誘発する因子の阻害剤
探索のためのバイオ計測系の開発に関する研究

研究代表者　太田　力　国立がん研究センター・ユニット長

</div>

研究要旨

我々は実に30%以上の非小細胞肺癌において転写因子Nrf2の異常活性化によって薬剤解毒酵素や薬剤排出ポンプ蛋白質の遺伝子が過剰発現され、抗癌剤抵抗性を示すことを見出した。従って、肺癌の抗癌剤抵抗性に関与する蛋白質の過剰発現を直接誘導している転写因子を分子標的とした阻害物質が開発出来れば、この阻害剤を抗癌剤補助薬として使用することで効果的な化学療法の実現が期待される。そこで、本研究では肺癌の抗癌剤抵抗性に直接関与する転写因子Nrf2を分子標的とした阻害物質探索を製薬会社との共同開発を可能にするバイオ計測系の構築を目的としている。本年度は、転写因子Nrf2の異常活性化癌細胞株を用いたバイオ計測系の開発を行った。

研究分担者
五十嵐　美徳
国立がん研究センター・主任研究員

A．研究目的

　肺癌の約8割を占める非小細胞肺癌に対する既存の抗癌剤の効果は未だ不十分であり、その原因に関してはよくわかっていなかった。我々は転写因子Nrf2の異常活性化によって薬剤解毒酵素や薬剤排出ポンプ蛋白質の遺伝子が過剰発現され、抗癌剤抵抗性を示すことを見出した。従って、肺癌の抗癌剤抵抗性に関与する蛋白質の過剰発現を直接誘導している転写因子を分子標的とした阻害物質が開発出来れば、この阻害剤を補助薬として使用することで効果的な化学療法の実現と肺癌の予後延長および死亡率減少が期待される。そこで、本研究では肺癌の抗癌剤抵抗性に直接関与する転写因子Nrf2を分子標的とした阻害物質探索を製薬会社との共同開発を可能にするバイオ計測系の構築を目的とした。

B. 研究方法

昨年度、転写因子 Nrf2 の活性抑制効果を示す 2 種類の低分子化合物を得た。今年度は、上記低分子化合物のがん細胞株への効果を検証した。また、転写因子 Nrf2 異常活性化肺癌細胞株をマウスの皮下に導入し、移植可能か検証した。さらに、転写因子 Nrf2 の機能領域の構造を解析する目的でリコンビナント Nrf2 蛋白質の精製および結晶化を試みた。

（倫理面への配慮）本研究の実施に当たっては「ヒトゲノム・遺伝子解析研究に関する倫理指針」に従い、国立がん研究センター遺伝子解析研究倫理審査委員会において審査を受け理事長の承認を得て実施している。また、動物を用いた解析は「厚生労働省の所管する実施機関における動物実験等の実施に関する基本指針」に従い実施した。

C. 研究成果

転写因子 Nrf2 の転写活性化能を抑制する効果は 100uM の濃度の化合物を 24 時間作用させて検証することが出来た。そこで、100 uM、10 uM、1 uM の濃度で、細胞増殖能に与える影響を検証したところ、1 uM の濃度でも細胞生存率が数％となり、かなり細胞毒性の高いことがわかった。そこで、化合物の濃度を nM オーダーで細胞に作用させたところ、Nrf2 が正常な肺癌細胞株と同程度の細胞増殖抑制効果が出てしまうことがわかった。そこで、nM オーダーでの Nrf2 転写抑制能を測定したところ、転写抑制能は全く検出することが出来なかった。以上の解析結果より、見出した低

分子化合物は Nrf2 転写抑制能を持つが、細胞毒性を示す活性が高いため、Nrf2 転写抑制能を示す濃度での細胞増殖抑制効果が検出できないことがわかった。また、転写因子 Nrf2 異常活性化肺癌細胞株をマウスの皮下に導入し、3 種類の細胞株が移植可能であることがわかった。さらに、大腸菌を用いて作成したリコンビナント Nrf2 蛋白質および MafG 蛋白質（Nrf2 とヘテロダイマーを形成する因子）を大量に得た。これら蛋白質を用いて、結晶化を進めている。

D. E 考察・結論

転写因子 Nrf2 の阻害効果を示す低分子化合物は毒性が高いため、癌細胞株への効果を検証することは出来なかった。今後、見出している低分子化合物の類縁体を収集・解析し、Nrf2 の阻害効果を保持するが、細胞毒性は低い化合物を探索する。また、将来、阻害効果をマウスで検証可能な Nrf2 異常活性化肺癌細胞株を見出したので、今後、利用していきたい。さらに、Nrf2-MafG 蛋白質の結晶化を成功させ、構造解析を進めて行きたい。

F. 健康危険情報

なし。

G. 研究発表

分担研究報告書に記載。

H. 知的財産権の出願・登録状況

分担研究報告書に記載。

別紙4

厚生労働科学研究費補助金（創薬基盤推進研究事業）

分担研究報告書

肺癌における抗癌剤抵抗性を誘発する因子の阻害剤探索のための
細胞を用いたバイオ計測系の開発に関する研究

研究代表者　太田　力　国立がん研究センター・ユニット長

研究要旨

本研究では肺癌の抗癌剤抵抗性に直接関与する転写因子 Nrf2 を分子標的とした阻害物質探索を
製薬会社との共同開発を可能にする細胞を用いたバイオ計測系の構築を目的としている。本年
度は、構築したバイオ計測系を用いて、スモールスケール（1万種）でのスクリーニングを行い、
昨年度得られた転写因子 Nrf2 の阻害活性能をもつ2種類の低分子化合物の癌細胞株における効
果の検証を行った。

A. 研究目的

　本研究では肺癌の抗癌剤抵抗性に直接関与
する転写因子 Nrf2 を分子標的とした阻害物
質探索を製薬会社との共同開発を可能にする
細胞を用いたバイオ計測系の構築およびバイ
オ計測系の検証を目的とした。

B. 研究方法

　昨年度、転写因子 Nrf2 の異常活性化癌細胞
株を用いて Nrf2 の阻害効果を示す低分子化
合物を見出した。そこで、これら化合物の癌
細胞株への効果を検証した。方法は、2 種類
の転写因子 Nrf2 の異常活性化癌細胞株個を
6cm プレートに播き、濃度の異なる化合物を

加え、3 日毎に培地交換（その度に化合物を
添加）を行い培養を行う。12 日後にコロニー
数をかぞえ、化合物の添加していない細胞
（DMSO のみ添加）でのコロニー数を 100 とし
て、細胞生存率を測定した。また、ネガティ
ブコントロールとして、転写因子 Nrf2 の正常
癌細胞株を用いた。

（倫理面への配慮）

本研究の実施に当たっては「ヒトゲノム・遺
伝子解析研究に関する倫理指針」に従い、国
立がん研究センター遺伝子解析研究倫理審査
委員会において審査を受け理事長の承認を得
て実施している。

C. 研究成果

E.　研究成果

　転写因子 Nrf2 の転写活性化能を抑制する効果は100uMの濃度の化合物を24時間作用させて検証することが出来た。そこで、100 uM、10 uM、1 uM および 0 uM の濃度で、細胞増殖能に与える影響を検証したところ、1 uM の濃度でも細胞生存率が数％となり、かなり細胞毒性の高いことがわかった。そこで、化合物の濃度を数百 nM オーダーで細胞に作用させたところ、Nrf2 が正常な肺癌細胞株と同程度の細胞増殖抑制効果が出てしまうことがわかった。そこで、数百 nM オーダーでのNrf2転写抑制能を測定したところ、転写抑制能は全く検出することが出来なかった。以上の解析結果より、見出した低分子化合物はNrf2転写抑制能を持つが、細胞毒性を示す活性が高いため、Nrf2転写抑制能を示す濃度での細胞増殖抑制効果が検出できないことがわかった。

　次に、転写因子Nrf2の転写活性化能を抑制する低分子化合物の類縁体化合物を入手し、Nrf2の転写活性化能を抑制する能力のある化合物を探索したところ、Nrf2の転写活性化能を抑制する低分子化合物を数種類得た。

D. E 考察・結論

　昨年度見出した転写因子 Nrf2 の阻害効果を示す低分子化合物は細胞毒性が高く、Nrf2の阻害効果を示す濃度における癌細胞株への効果を検証することは出来なかった。最近、Nrf2の阻害効果を示す低分子化合物の類縁体（低分子化合物）を収集し、Nrf2の阻害効果を示す化合物を2種類得た。今後、これら低

分子化合物の細胞毒性を検証し、Nrf2異常活性化肺癌細胞株に及ぼす影響を調べる予定である。また、1 万種類の低分子化合物ライブラリーから、実際転写因子 Nrf2 の阻害物質のスクリーニングが可能であることが判明したので、今後、転写因子 Nrf2 の阻害物質のスクリーニングを製薬会社との共同研究として進めて行く予定である。

F. 健康危険情報
　なし。

G. 研究発表

1.　論文発表
　なし。

2.　学会発表
1. 宮本麻美子、太田力. 滑膜肉腫の治療法の探索. 第 71 回日本癌学会学術総会、2012.

2. 　山本悠貴、太田力. 一塩基多型によるDNA 修復蛋白質の活性低下. 第 71 回日本癌学会学術総会、2012.

3. 　山本悠貴、太田力. 一塩基多型によるDNA 修復蛋白質の活性低下. 第 35 回日本分子生物学会年会、2012.

H. 知的財産権の出願・登録状況
　なし。

厚生労働科学研究費補助金（創薬基盤推進研究事業）

分担研究報告書

肺癌における抗癌剤抵抗性を誘発する因子の阻害剤探索のための

細胞を用いたバイオ計測系の開発に関する研究

研究分担者 五十嵐 美徳　　国立がん研究センター・主任研究員

研究要旨

本研究では肺癌の抗癌剤抵抗性に直接関与する転写因子 Nrf2 を分子標的とした阻害物質探索を製薬会社との共同開発を可能にする細胞を用いたバイオ計測系の構築を目的としている。本年度は、マウスに移植して利用できる転写因子 Nrf2 の異常活性化癌細胞株の探索、および、転写因子 Nrf2 の構造解析のための蛋白質大量発現・精製を行った。

A. 研究目的

　本研究では肺癌の抗癌剤抵抗性に直接関与する転写因子 Nrf2 を分子標的とした阻害物質探索を製薬会社との共同開発を可能にするマウスを用いたバイオ計測系の構築、および、転写因子 Nrf2 の構造解析のための蛋白質大量発現・精製を目的とした。

B. 研究方法

　新規に転写因子 Nrf2 の異常活性化癌細胞株を探索した。方法は、肺癌細胞株 15 種類を入手し、RT-PCR 法を用いて転写因子 Nrf2 の下流遺伝子の発現量を解析した。次に、Nrf2 の下流遺伝子の発現量が高いことが確認された細胞株に NRF2 遺伝子特異的な siRNA を導入して NRF2 遺伝子の発現をノックダウンさせ

場合に、Nrf2 の下流遺伝子の発現量が低下する細胞を選択した。また、転写因子 Nrf2 の構造解析のため、DNA 結合領域を大腸菌を用いて発現させ、アフニティークロマトグラフィーを用いて精製し、結晶化を試み。

（倫理面への配慮）

本研究の実施に当たっては「ヒトゲノム・遺伝子解析研究に関する倫理指針」に従い、国立がん研究センター遺伝子解析研究倫理審査委員会において審査を受け理事長の承認を得て実施している。また、動物を用いた解析は「厚生労働省の所管する実施機関における動物実験等の実施に関する基本指針」に従い実施した。

C．研究成果

　肺癌細胞株 15 種類で転写因子 Nrf2 の下流遺伝子の発現が比較的高い細胞は 4 種類見出された。さらに、これら 4 種類の細胞株に NRF2 遺伝子特異的な siRNA を導入して NRF2 遺伝子の発現をノックダウンさせたところ、3 種類の細胞株で転写因子 Nrf2 の下流遺伝子の発現量が低下することがわかった。次に、これら 3 種類の細胞株をマウスの皮下に導入し、移植可能か検証した。各細胞株の細胞数を千個から 10 万個をマウスの皮下に導入し、腫瘍の形成を観察したところ、2 種類の細胞が腫瘍を形成することがわかった。さらに、これら 2 種類の細胞株の足場依存のコロニー形成能を調べたところ、マウスでの腫瘍形成能と相関することがわかった。また、大腸菌内でNrf2-MafG ヘテロダイマーを形成させるため、His-Nrf2 と GST-MafG を同時に大腸菌内で発現させた。その結果、効率よく大腸菌内でNrf2-MafG ヘテロダイマーが形成され、ニッケルカラムおよび GST カラムを用いて大量のNrf2-MafG ヘテロダイマー複合体蛋白質を得た。

D．E．考察・結論

　将来、見出される阻害物質をマウスで検証するためには、マウスに移植可能な転写因子 Nrf2 異常活性化肺癌細胞株が必要となるが、今年度 2 株の癌細胞株を得ており、昨年度得た 1 株と合わせて合計 3 株を得た。今後、転写因子 Nrf2 の阻害物質が得られた場合、これら 3 株を用いて、動物実験に応用して行きたいと思っている。また、Nrf2、MafG の蛋白質に関しては、Nrf2 と MafG を同時に大腸菌内で発現させることによって、Nrf2-MafG ヘテロダイマーを大量に精製できた。現在、これらの精製票品を用いて蛋白質複合体の結晶化を試みている。

F．健康危険情報

　なし。

G．研究発表

1．論文発表

1. Yamazaki T, Aoki K, Heike Y, Kim SW, Ochiya T, Wakeda T, Hoffman RM, Takaue Y, Nakagama H, **Ikarashi Y**. Real-time in vivo cellular imaging of graft-versus-host disease and its reaction to immunomodulatory reagents. **Immunol Lett. 144, 33-40 (2012).**

2．学会発表

1. 五十嵐美徳、平家勇司. NKT 細胞リガンドによる同種造血幹細胞移植後のドナー細胞の生着抑制. 第 71 回 日本癌学会学術総会 2012.

H．知的財産権の出願・登録状況

　なし。

別紙 5

研究成果の刊行に関する一覧表

雑誌

発表者氏名	論文タイトル名	発表誌名	巻号	ページ	出版年
Yamazaki T, Ikarashi Y., et al.	Real-time in vivo cellular imaging of graft-versus-host disease and its reaction to immunomodulatory	Immunol Lett.	144	33-40	2012年

Real-time *in vivo* cellular imaging of graft-*versus*-host disease and its reaction to immunomodulatory reagents

Takahiro Yamazaki[a], Kazunori Aoki[a], Yuji Heike[b], Sung-Won Kim[b], Takahiro Ochiya[c], Takako Wakeda[b], Robert M. Hoffman[d,e], Yoichi Takaue[b,g], Hitoshi Nakagama[f], Yoshinori Ikarashi[a,h,*]

[a] *Division of Gene and Immune Medicine, National Cancer Center Research Institute, 5-1-1, Tsukiji, Chuo-ku, Tokyo 104-0045, Japan*
[b] *Department of Hematology and Hematopoietic Stem Cell Transplantation, National Cancer Center Hospital, Japan*
[c] *Division of Molecular and Cellular Medicine, National Cancer Center Research Institute, Japan*
[d] *AntiCancer, Inc., 7917 Ostrow Street, San Diego, CA 92111, United States*
[e] *Department of Surgery, University of California San Diego, 200 West Arbor Drive, San Diego, CA 92103-8220, United States*
[f] *Division of Cancer Development System, National Cancer Center Research Institute, Japan*
[g] *Institute for Research, St. Luke's International Hospital, Akashi-cho, Chuo-ku, Tokyo104-8560, Japan*
[h] *Central Animal Division, National Cancer Center Research Institute, Japan*

ARTICLE INFO

ABSTRACT

Visualizing the in vivo dynamics of individual donor cells after allogeneic hematopoietic stem cell transplantation (HSCT) will enable deeper understanding of the process of graft-*versus*-host disease (GVHD) and graft-*versus*-leukemia (GVL). In this study, using non-invasive in vivo fluorescence imaging of the ear pinna, we successfully visualized green fluorescent protein (GFP) donor cells at the single cell level in the skin. This imaging model enabled visualization of the movement of GFP cells into blood vessels in real time after allogeneic HSCT. At day 1, a few donor cells were detected, and the movement of donor cells in blood vessels was readily observed at day 4. Early donor cell infiltration into non-lymphoid tissue was increased by treatment with croton oil, as an inflammatory reagent. Treatment with dexamethasone, as an anti-inflammatory reagent, suppressed donor cell infiltration. The in vivo cellular fluorescence imaging model described here is a very useful tool for monitoring individual donor cells in real-time and for exploring immunomodulatory reagents for allogeneic HSCT, as well as for understanding the mechanism of GVHD.

© 2012 Elsevier B.V. All rights reserved.

1. Introduction

Allogeneic hematopoietic stem cell transplantation (HSCT) is an effective cell-therapy for hematological malignancies [1–3]. Donor immune cells in the graft promote the elimination of leukemic cells known as graft-*versus*-leukemia (GVL). However, donor T cells, which recognize major and minor histocompatibility antigenic disparity between donor and host, trigger host-tissue damage, termed graft-*versus*-host disease (GVHD), which is a potentially fatal adverse reaction of allogeneic HSCT [2–5]. The control of GVHD is one of the major challenges in clinical oncology. *In vivo* imaging techniques using green fluorescent protein (GFP) or luciferase transgenic mice as donors have been used to visualize the dynamics of donor immune cells after allogeneic HSCT. Imaging has demonstrated that donor T cells initially migrate into secondary lymphoid tissues where they undergo activation and proliferation and enter target tissues, such as the liver, gastrointestinal tract and skin [6–11].

In vivo fluorescence imaging has been widely used for whole-body visualization in real time and multiple colors [12–20]. Further, single cell imaging can visualize lymphocyte trafficking in lymphatic and blood vessels [21,22], as well as cell-to-cell interaction in lymph nodes [23,24]. In a GVHD mouse model, donor cells were tracked at the single-cell level *in vivo* [7,25].

In this study, using *in vivo* fluorescence imaging with cellular resolution, we evaluated the effects of immunomodulatory drugs on donor-cell migration at the single-cell level in non-lymphoid tissue such as ear pinna. It was thus possible to assess the effects of the drug, and have a control, in the same animal when the drug was painted on one ear pinna with the other serving as a control.

2. Materials and methods

2.1. Mice

Female C57BL/6-Tg (CAG-EGFP) mice (termed B6-GFP-Tg, H-$2^{b/b}$), ubiquitously expressing enhanced green fluorescence protein [26], and (C57BL/6NCrSlc × DBA/2CrSlc) F_1 (termed BDF1, H-$2^{b/d}$)

* Corresponding author at: Central Animal Division, National Cancer Center Research Institute, 5-1-1, Tsukiji, Chuo-ku, Tokyo 104-0045, Japan.
Tel.: +81 3452 2511x4452; fax: +81 3248 1631.
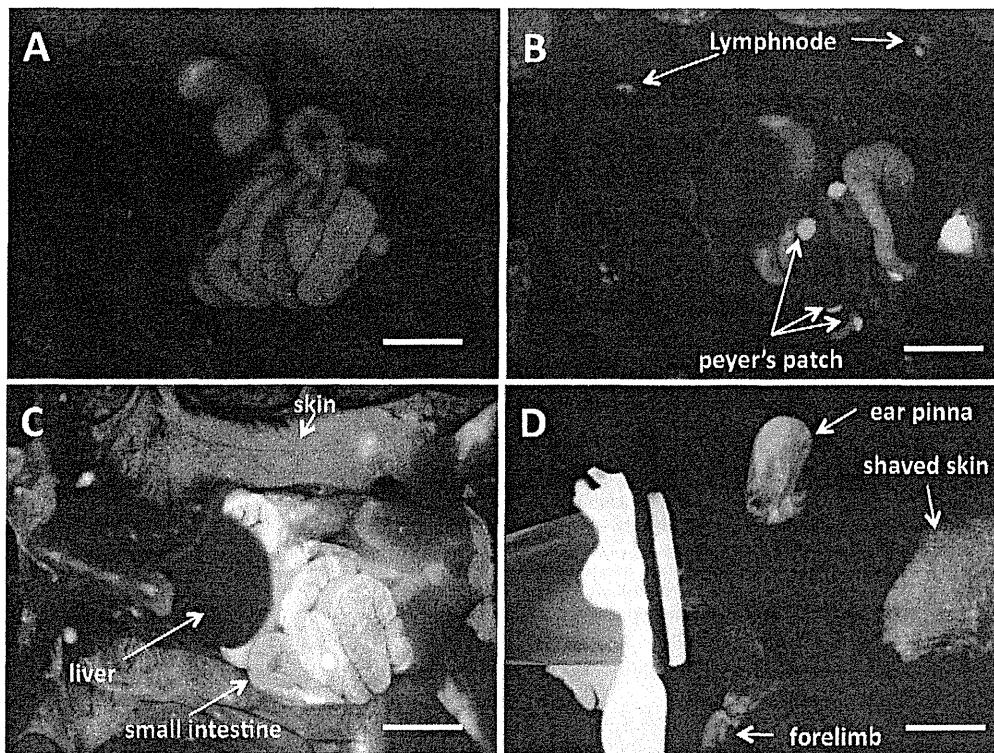*E-mail addresses:* yikarash@gan2.ncc.go.jp, yikarash@ncc.go.jp (Y. Ikarashi).

Fig. 1. *In vivo* fluorescence imaging of donor cells in opened mice after allogeneic HSCT. Spleen and bone marrow cells from B6-GFP-Tg donor mice were injected intravenously into BDF1 mice. (A–C) Mice were sacrificed and opened. GFP donor cells in whole body were visualized with the OV110 Small Animal Imaging System (A: control, B: 1 day, C: 14 days). (D) Thirty five days after transplantation, shaved mice were anesthetized and imaged with the OV110. Arrows indicate GFP+ cells in organs.

mice, were purchased from Japan SLC, Inc. (Hamamatsu, Japan). All mice were maintained in specific pathogen-free conditioned animal facilities at the National Cancer Center Research Institute. Mice between 8 and 12 weeks of age were used for all transplantation experiments. Animal studies were carried out according to the Guideline for Animal Experiments and approved by the committee for ethics of animal experimentation at the National Cancer Center.

2.2. Allogeneic HSCT mice model and treatment with immunomoduratory reagents

A mixture of 5×10^7 spleen cells and 5×10^6 bone marrow cells from B6-GFP-Tg mice was injected intravenously *via* the tail vein into untreated BDF1 mice as described previously [27,28]. Croton oil, used as an inflammatory regent, and dexamethasone, used as an anti-inflammatory reagent, were obtained from Sigma–Aldrich (St. Louis, MO). At 3 h or 7 days after allogeneic HSCT, the mice were painted on the right ear pinna with croton oil (acetone 1 µl/20 µl) or dexamethasone (acetone 0.5 µg/20 µl), respectively. As a control, the same mice were painted on the left ear pinna with 20 µl acetone alone.

2.3. Variable magnification in vivo fluorescence imaging

The OV110 Small Animal Imaging System (Olympus, Tokyo, Japan) with a cooled charge-coupled device CCD color camera and a GFP-bandpass filter, was used for non-invasive imaging from macro to micro [13]. The mice were anesthetized with isoflurane by inhalation, and sequentially imaged for the GFP donor cells in the ear pinna and shaved skin. Exposure times were

optimized and identical for each experiment. Video was acquired at 10 frames/s. All images and video were obtained with OV110 software. To assess the effects of drugs on donor cell infiltration after allogeneic HSCT, GFP donor cell infiltration in the ear pinna was quantitatively analyzed. GFP donor cells in the ear pinna were initially counted and calculated as the number of donor cells per mm^2. At later stages after transplantation, the fluorescence intensity of GFP was calculated with OV110 software. To avoid contamination of autofluorescence from hair, images were obtained from the hairless areas in the ear pinna. When video of the movement of GFP cells in the blood vessels was made, hair in the ear pinna was removed by epilation to avoid autofluorescence.

2.4. Donor cell imaging in tissue sections and immunofluorescence staining

Tissues were fixed with 4% paraformaldehyde in PBS at 4 °C for 1 h followed by transfer into 10% sucrose in PBS for 12–24 h and 20% sucrose in PBS over 12 h. The tissues were embedded into an O.C.T. compound (Miles Laboratory, IN), and quickly frozen in cold isopentane. For immunofluorescence staining, the frozen block was cut into 5 µm thick sections with a cryostat (Sakura Finetek Japan, Tokyo, Japan). The sections were air-dried and incubated with blocking solution (5% normal goat serum and 1% bovine serum albumin in PBS) for 30 min and then incubated overnight at 4 °C with anti-CD3ε (500A2, eBioscience, San Diego, CA). Sections were then incubated with Alexa Fluor 594-conjugated goat anti-rat IgG antibody (invitrogen) for 1 h at room temperature. After each incubation, sections were washed with PBS containing 0.01% Triton X. Sections were mounted with VECTASHIELD with DAPI
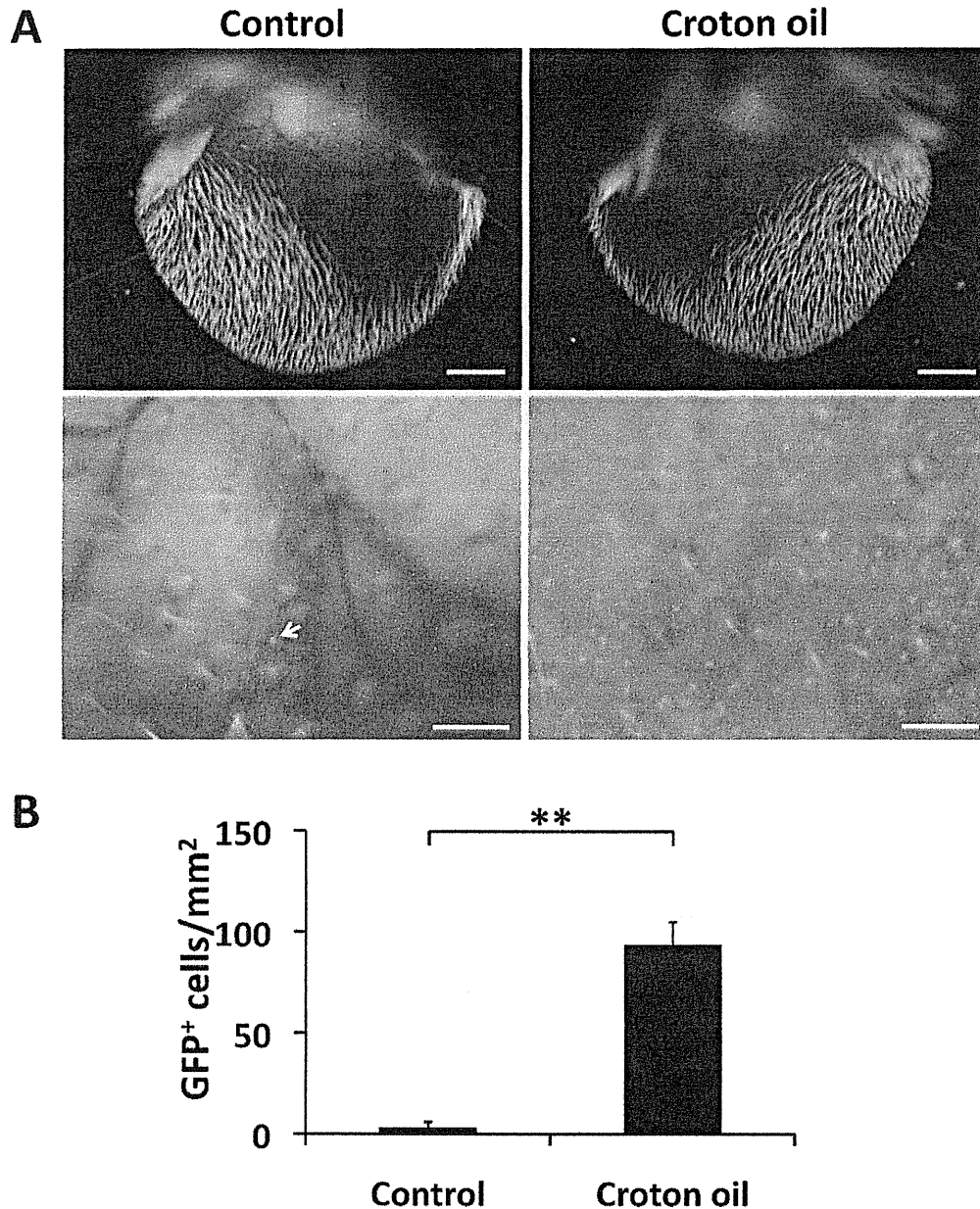
Fig. 2. Quantitative *in vivo* fluorescence imaging of donor cells in the ear pinna and the effects of inflammatory agents. (A) At 3 h after transplantation, croton oil (right panels) and acetone alone as a control (left panels), were painted on right and left ears, respectively. At day 1, GFP donor cells in the ear pinna were imaged. Low magnification images are in upper panels (scale bar, 2 mm) and high magnification images are in lower panels (scale bar, 250 μm.). Data are representative of 7 mice. (B) At day 1 after transplantation, GFP cells were counted in the ear pinna with high magnification and the number of GFP cells per 1 mm^2 was calculated. The data were from 13 fields from 5 mice and show mean ± SD. **$p < 0.01$. Arrow indicates GFP+ cell.

(Vector Laboratories, Inc., Burlingame, CA). The sections were observed under fluorescence microscopy (Eclipse E1000, Nikon, Tokyo, Japan) equipped with a QICAM FAST1394 CCD camera (QImage, Surrey, BC, Canada) and Meta Morph software (Universal Imaging Corp., Buckinghamshire, UK). In the tissue sections, the number of donor cells was quantitated by manually counting GFP cells.

2.5. Statistical analysis

The statistical significance of differences between experimental groups was determined using the Student's *t*-test.

3. Results

3.1. Fluorescence imaging of donor cells after allogeneic HSCT

Using a fluorescence macro–microscopic imaging system (OV110), we could clearly visualize GFP donor cell localization in mice with open abdomens (Fig. 1A–C). GFP fluorescence was easily distinguished from orange autofluorescence in the gastrointestinal tract (Fig. 1). Similar to previous reports [7], donor cells immediately localized to secondary lymphoid tissues and then infiltrated into the whole body in the allogeneic HSCT recipients. We readily detected GFP cells in the shaved skin, ear pinna and forelimb at day 35 after transplantation (Fig. 1D). GFP donor cells were also
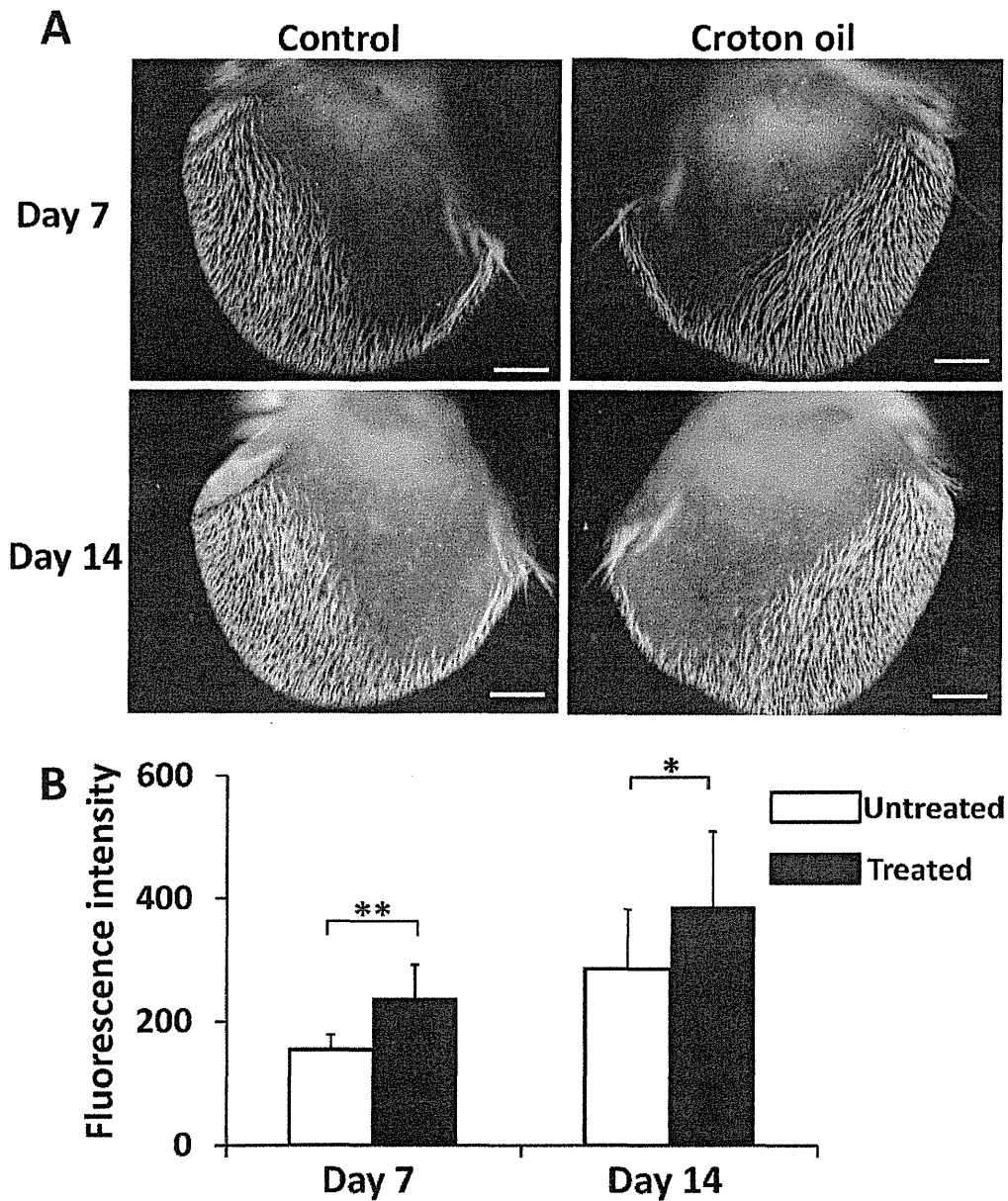
Fig. 3. *In vivo* imaging of exacerbation of donor cell infiltration by treatment with croton oil. (A) At 3 h after transplantation, croton oil (right panels) and acetone alone as control (left panels) were painted on right and left ears, respectively. At 7 (upper panels) and 14 (lower panels) days after transplantation, GFP donor cells in the ear pinna were imaged with the OV110 (scale bar, 2 mm.). Data are representative of 8–12 mice. (B) Fluorescence intensity of GFP was measured with the OV110 software. The data were from 8 mice and show mean ± SD. $*p < 0.05$, $**p < 0.01$.

detected in the liver, small intestine, lymphnode and Peyer's patch at the single-cell level in the dissected mice (data not shown).

3.2. Non-invasive in vivo fluorescence imaging of donor cells in the ear pinna at the single-cell level after allogeneic HSCT

To sequentially monitor donor cell infiltration after transplantation in the same mouse, we imaged the donor cells in the ear pinna. We determined whether donor cells could be non-invasively imaged in the ear pinna at the single-cell level. At day 1 after transplantation, donor cells were detectable at that site (Fig. 2A, lower left panel). Further, we could observe the movement of GFP donor cells into the blood vessels in the ear pinna. At day 4, GFP donor cells rapidly flowing, rolling or attaching to the vessels in the ear pinna were observed (supplemental video 1). These results indicate

that it is possible to non-invasively monitor the dynamics of donor cells in the skin at the single-cell level.

3.3. Imaging the efficacy of immunomodulatory agents

We assessed whether non-invasive *in vivo* fluorescence imaging would be useful for screening immunomodulatory drugs for GVHD in the skin, which is a major target for GVHD. First, we tested the effect of croton oil as an inflammation stimulator after allogeneic HSCT. At 3 h after transplantation, the mice were painted with croton oil on the right ear with the left ear serving as a control. At day 1 after transplantation, increased infiltration of donor cells was clearly observed at high magnification in the ear pinna treated with croton oil (Fig. 2A). Moreover, it was possible to count GFP cells in the field and calculate the number of

A Control Croton oil

Day 7
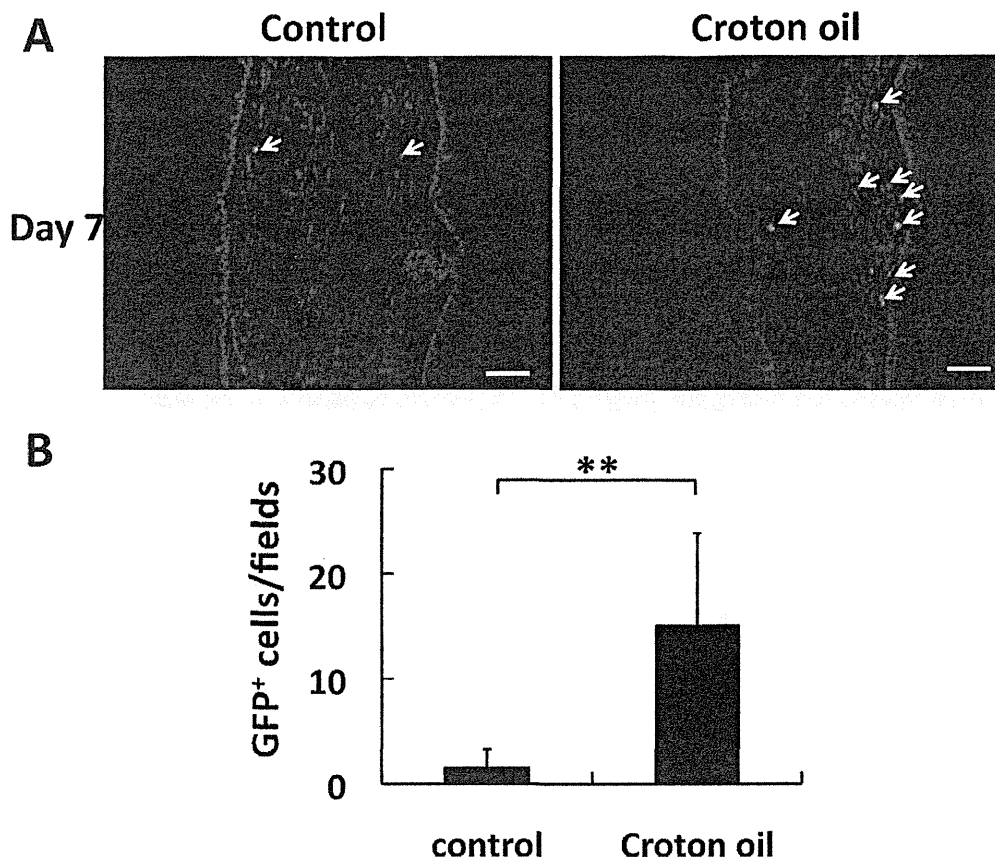
B

GFP⁺ cells/fields

Fig. 4. Quantitative analysis of donor cell infiltration in frozen sections. (A) At 3 h after transplantation, croton oil (right panels) and acetone alone as control (left panels) were painted on right and left ears, respectively. At day 7 after transplantation, GFP cells in the frozen tissue sections were observed by fluorescence microscopy (scale bar, 50 μm.). (B) At day 7 after transplantation, GFP cells were counted in the frozen sections. Data were from 20 fields from 3 mice and show mean ± SD. **$p < 0.01$.

donor cells per area. At day 1, a few GFP cells were observed in the control ear pinna, whereas approximately 90 GFP cells per mm² pinna accumulated in the ear after treatment with croton oil (Fig. 2B).

At 7 and 14 days after transplantation, donor cell infiltration was obviously increased in the ear pinna by treatment with croton oil (Fig. 3A). Since counting the number of infiltrating donor cells with the OV110 was difficult, due to the accumulation of many donor cells in the ear pinna, we calculated the fluorescence intensity per area using OV110 software. The analysis showed that donor cell infiltration was significantly increased in croton-oil-treated ear pinna at 7 and 14 days after transplantation (Fig. 3B). To validate the quantification of donor cell infiltration using *in vivo* imaging, we compared it with the conventional method of counting the number of GFP cells in frozen sections. Similar to *in vivo* imaging, GFP cells were found to be significantly increased in the frozen sections from croton-oil-treated tissue (Fig. 4). These results indicated that non-invasive *in vivo* fluorescence imaging is able to evaluate the effects of immunomodulatory drugs on donor-cell infiltration after allogeneic HSCT.

In order to determine whether anti-inflammatory drugs suppress donor-cell infiltration in allogeneic HSCT recipients, dexamethasone, as an anti-inflammatory drug, was painted on the right ear at day 7 after transplantation and monitored for alteration of donor cell infiltration (Fig. 5A). *In vivo* fluorescence imaging revealed that dexamethasone could significantly suppress donor cell infiltration at 14 days after transplantation (Fig. 5).

3.4. Identification of infiltrating cell subsets using immunofluorescence staining

Next, we identified the subsets of infiltrating cells. At day 7 after transplantation, CD3⁺ and GFP cells were observed in the croton oil-treated ear pinna, using immunofluorescence staining (Fig. 6A and B). At day 14, dexamethasone treatment suppressed GFP-cell and CD3⁺-cell infiltration in the skin (Fig. 6C and D). GFP⁻ CD3⁺-cells derived from the host were also observed (Fig. 6B and C).

4. Discussion

An analysis of the *in vivo* dynamics of donor cells is useful for understanding the process of allogeneic HSCT, such as GVHD, GVL and reconstitution of hematopoietic and immune systems. *In vivo* imaging techniques are suitable for an analysis of the dynamics of donor cells after allogeneic HSCT and have revealed their migration and expansion patterns [6–11]. In the present report, we showed that a non-invasive *in vivo* macro–micro fluorescence imaging system is a very useful tool for monitoring donor cells at the single cell level and in real time, and for exploring inhibitory drugs and exacerbating factors of GVHD.

The skin is a major target tissue of GVHD and cutaneous involvement is the most frequent GVHD manifestation [4,5]. To monitor the skin after induction of GVHD, it was possible to non-invasively and sequentially visualize individual GFP donor cells in mice [3]. Further, using the ear pinna, GFP donor cells infiltrating the immunomodulatory drug-treated ear were able to be compared
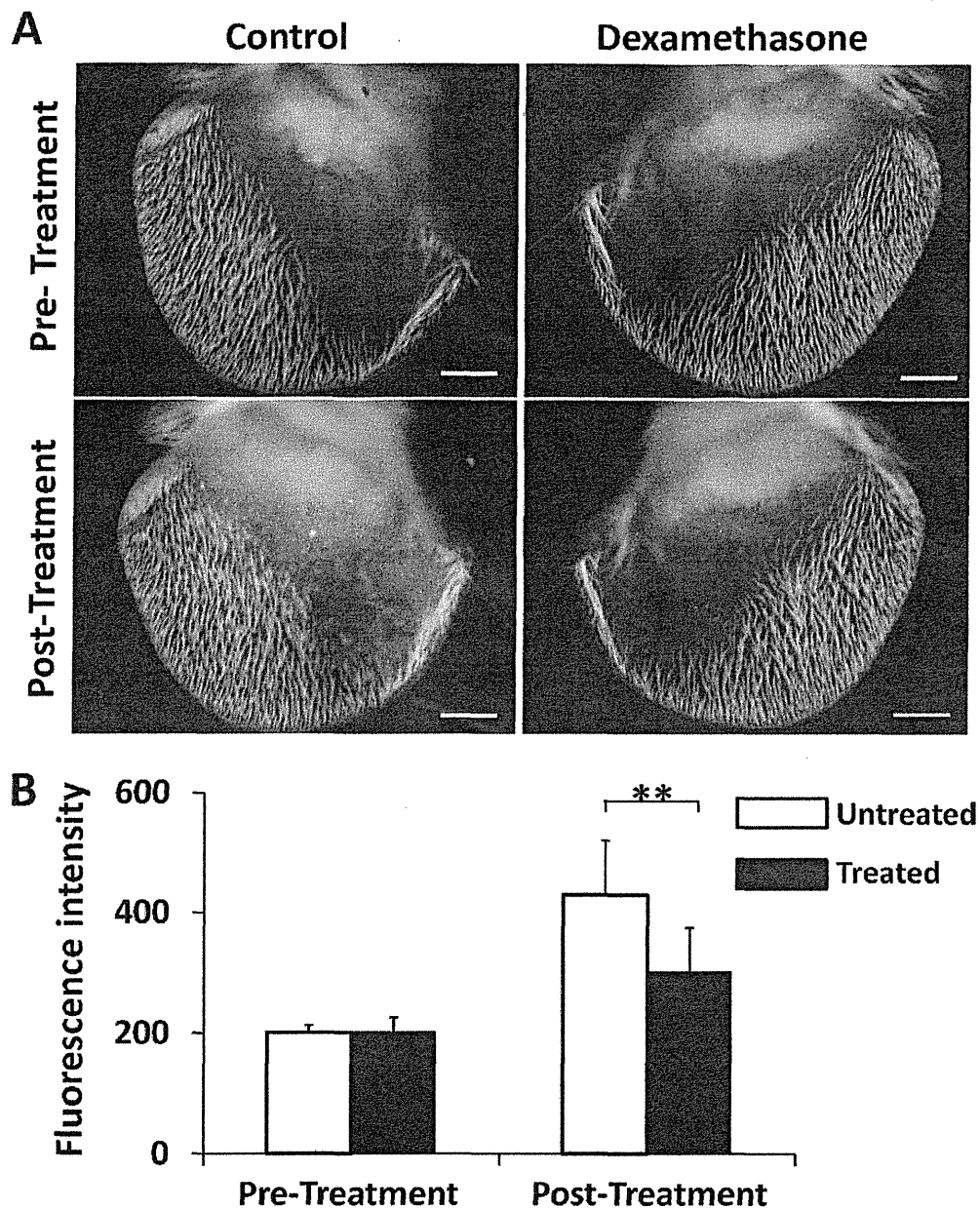
Fig. 5. The effect of dexamethasone on donor cell infiltration. (A) At 7 days after transplantation, dexamethasone (right panels) and acetone alone as control (left panels) were painted on right and left ears, respectively. Before treatment (upper panels) and at day 14 after transplantation (lower panels), GFP donor cells in the ear pinna were imaged with the OV110 (scale bar, 2 mm.). Data are representative of 8 mice. (B) Fluorescence intensity of GFP was measured with the OV110 software. The data were from 7 mice and show mean ± SD. **$p < 0.01$.

with those in the untreated ear in the same animal, enabling the determination of the effects of immunomodulatory drugs for skin GVHD at the local level. It has been previously reported that donor cells could be detected in lymph nodes at 6 h [7,29]. Using fluorescence macro–microscopy, we could image individual GFP donor cells in whole ear pinna including the trafficking of donor cells in the blood vessels.

Fluorescence imaging as well as conventional methods for counting GFP cells in frozen sections revealed that GFP cell infiltration was significantly increased by croton oil. The advantages of *in vivo* fluorescence imaging are its ability to count individual GFP cells in the large area of the ear pinna and evaluate the degree of donor cell infiltration in real-time without having to make frozen sections. Moreover, we could sequentially monitor GFP cells in the same animal to compare treated and untreated ear pinna in the

same mouse to evaluate the effects of drugs on skin GVHD in real time.

Regarding selectivity of donor cells recruitment, Panoskaltsis-Mortari et al. [7] reported that donor cells were observed in lymphoid tissues at 7 days after transplantation in syngeneic mice, but they are not present or present only at low levels in target tissues such as skin, liver and lung compared with allogeneic mice. Therefore, we suggest that donor cells which are observed in the skin in our report are selectively recruited.

Immunofluorescence staining analysis enabled identification of the infiltrating donor and host cell subsets in the lesions and increased our understanding of the pathogenesis of GVHD. Immunofluorescence staining revealed that at day 1 after transplantation, GFP cells detected in the ear pinna treated with croton oil were Gr1+ cells, and that a large number of recipient Gr1+ cells
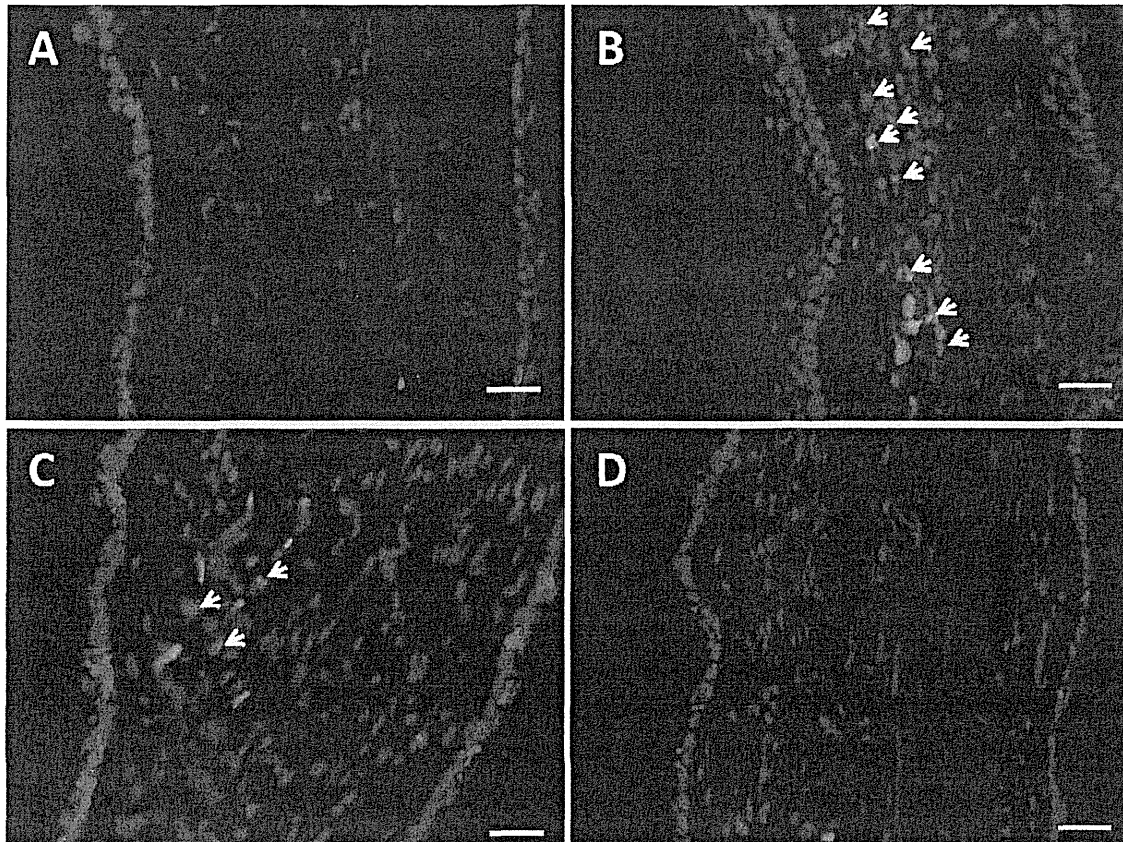
Fig. 6. Identification of infiltrating donor cell subsets using immunofluorescence staining. (A and B) At 3 h after transplantation, croton oil (B) and acetone alone as control (A) were painted on right and left ears, respectively and analyzed at day 7 after transplantation. (C and D) At day 7 after transplantation, dexamethasone (D) and acetone alone as control (C) were painted on right and left ears, respectively and analyzed at day 14 after transplantation. (A–D) Frozen sections of ear pinna were stained with CD3 monoclonal antibody and GFP and CD3$^+$ cells were observed by fluorescence microscopy (scale bar, 100 μm). Arrows indicate GFP CD3$^+$ cells (donor T cells). Data are representative of 3 mice.

(GFP$^-$ cells) also infiltrated (data not shown). Croton oil stimulation is known to induce neutrophil accumulation [30,31]; therefore early recruitment of both donor- and recipient-type Gr1$^+$ cells could be elicited by croton oil stimulation rather than allogeneic responses. Activated neutrophils produce several chemkines such as CXCL9, CXCL10 and CXCL11 which attract CXCR3-expressing T cells [32–34]. Furthermore, on day 3 after transplantation, CXCL10 and CXCL11 produced in target tissues, directed the early recruitment of activated CXCR3-expressing donor T cells [35]. Our results showed that increased donor cell infiltration was observed in the ear pinna treated with croton oil after transplantation. We suggest that increased donor cell infiltration could be dependent not only on inflammatory responses by croton oil, but on allogeneic responses as well. Immunofluorescence staining of CD3, infiltrating T cells showed they were both donor and recipient. In this study, we used non-myeloablative allogeneic HSCT mouse models. Recipient immune cells were not depleted by conditioning; thus, recipient T cells might be involved in the lesions [22]. Treatment with corticosteroid alleviates skin GVHD, which was demonstrated by fluorescence imaging in real time.

In conclusion, non-invasive and single cell *in vivo* imaging using a fluorescence macro–microscope is very useful for drug screening for early- and late-stage GVHD in real time.

Acknowledgments

Appendix A. Supplementary data

Supplementary data associated with this article can be found, in the online version, at doi:10.1016/j.imlet.2012.03.004.

References

[1] Horowitz MM, Gale RP, Sondel PM, Goldman JM, Kersey J, Kolb HJ, et al. Graft-versus-leukemia reactions after bone marrow transplantation. Blood 1990;75:555–62.
[2] Appelbaum FR. Haematopoietic cell transplantation as immunotherapy. Nature 2001;411:385–9.
[3] Welniak LA, Blazar BR, Murphy WJ. Immunobiology of allogeneic hematopoietic stem cell transplantation. Annu Rev Immunol 2007;25:139–70.
[4] Ferrara JL, Levine JE, Reddy P, Holler E. Graft-versus-host disease. Lancet 2009;373:1550–61.
[5] Shlomchik WD. Graft-versus-host disease. Nat Rev Immunol 2007;7:340–52.
[6] Negrin RS, Contag CH. In vivo imaging using bioluminescence: a tool for probing graft-versus-host disease. Nat Rev Immunol 2006;6:484–90.
[7] Panoskaltsis-Mortari A, Price A, Hermanson JR, Taras E, Lees C, Serody JS, et al. In vivo imaging of graft-versus-host-disease in mice. Blood 2004;103:3590–8.
[8] Stelljes M, Hermann S, Albring J, Köhler G, Löffler M, Franzius C, et al. Clinical molecular imaging in intestinal graft-versus-host disease: mapping of disease activity, prediction, and monitoring of treatment efficiency by positron emission tomography. Blood 2008;111:2909–18.
[9] Taylor PA, Ehrhardt MJ, Lees CJ, Panoskaltsis-Mortari A, Krieg AM, Sharpe AH, et al. TLR agonists regulate alloresponses and uncover a critical role for donor APCs in allogeneic bone marrow rejection. Blood 2008;112:3508–16.

[10] Beilhack A, Schulz S, Baker J, Beilhack GF, Wieland CB, Herman EI, et al. In vivo analyses of early events in acute graft-versus-host disease reveal sequential infiltration of T-cell subsets. Blood 2005;106:1113–22.

[11] Nguyen VH, Zeiser R, Dasilva DL, Chang DS, Beilhack A, Contag CH, et al. In vivo dynamics of regulatory T-cell trafficking and survival predict effective strategies to control graft-versus-host disease following allogeneic transplantation. Blood 2007;109:2649–56.

[12] Hoffman RM. The multiple uses of fluorescent proteins to visualize cancer in vivo. Nat Rev Cancer 2005;5:796–806.

[13] Yamauchi K, Yang M, Jiang P, Xu M, Yamamoto N, Tsuchiya H, et al. Development of real-time subcellular dynamic multicolor imaging of cancer-cell trafficking in live mice with a variable-magnification whole-mouse imaging system. Cancer Res 2006;66:4208–14.

[14] Hoffman RM, Yang M. Whole-body imaging with fluorescent proteins. Nat Protoc 2006;1:1429–38.

[15] Yamauchi K, Yang M, Jiang P, Yamamoto N, Xu M, Amoh Y, et al. Real-time in vivo dual-color imaging of intracapillary cancer cell and nucleus desformation and migration. Cancer Res 2005;65:4246–52.

[16] Hoffman RM. In vivo real-time imaging of nuclear-cytoplasmic dynamics of dormancy, proliferation and death of cancer cells. APMIS 2008;116:716–29.

[17] Yamauchi K, Yang M, Hayashi K, Jiang P, Yamamoto N, Tsuchiya H, et al. Induction of cancer metastasis by cyclophosphamide pretreatment of host mice: an opposite effect of chemotherapy. Cancer Res 2008;68:516–20.

[18] Yang M, Li L, Jiang P, Moossa AR, Penman S, Hoffman RM. Dual-color fluorescence imaging distinguishes tumor cells from induced host angiogenic vessels and stromal cells. Proc Natl Acad Sci U S A 2003;100:14259–62.

[19] Yang M, Reynoso J, Jiang P, Li L, Moossa AR, Hoffman RM. Transgenic nude mouse with ubiquitous green fluorescent protein expression as a host for human tumors. Cancer Res 2004;64:8651–6.

[20] Hasegawa A, Hayashi K, Kishimoto H, Yang M, Tofukuji S, Suzuki K, et al. Color-coded real-time cellular imaging of lung T-lymphocyte accumulation and focus formation in a mouse asthma model. J Allergy Clin Immunol 2010;125:461–8.

[21] Miller MJ, Wei SH, Cahalan MD, Parker I. Autonomous T cell trafficking examined in vivo with intravital two-photon microscopy. Proc Natl Acad Sci U S A 2003;100:2604–9.

[22] Mempel TR, Scimone ML, Mora JR, von Andrian UH. In vivo imaging of leukocyte trafficking in blood vessels and tissues. Curr Opin Immunol 2004;16:406–17.

[23] Stoll S, Delon J, Brotz TM, Germain RN. Dynamic imaging of T cell-dendritic cell interaction in lymph nodes. Science 2002;296:1873–6.

[24] Mempel TR, Henrickson SE, Von Andrian UH. T-cell priming by dendritic cells in lymph nodes occurs in three distinct phases. Nature 2004;427:154–9.

[25] Chakraverty R, Côté D, Buchli J, Cotter P, Hsu R, Zhao G, et al. An inflammatory checkpoint regulates recruitment of graft-versus-host reactive T cells to peripheral tissues. J Exp Med 2006;203:2021–31.

[26] Okabe M, Ikawa M, Kominami K, Nakanishi T, Nishimune Y. 'Green mice' as a source of ubiquitous green cells. FEBS Lett 1997;407:313–9.

[27] Ikarashi Y, Matsumoto Y, Omata S, Fujiwara M. Recipient-derived T cells participate in autoimmune-like hepatic lesions induced by graft-versus-host reaction. Autoimmunity 1995;20:121–7.

[28] Kuwatani M, Ikarashi Y, Iizuka A, Kawakami C, Quinn G, Heike Y, et al. Modulation of acute graft-versus-host disease and chimerism after adoptive transfer of in vitro-expanded invariant Valpha14 natural killer T cells. Immunol Lett 2006;106:82–90.

[29] Taylor PA, Ehrhardt MJ, Lees CJ, Tolar J, Weigel BJ, Panoskaltsis-Mortari A, et al. Insights into the mechanism of FTY720 and compatibility with regulatory T cells for the inhibition of graft-versus-host disease (GVHD). Blood 2007;110:3480–8.

[30] Mizgerd JP, Bullard DC, Hicks MJ, Beaudet AL, Doerschuk CM. Chronic inflammatory disease alters adhesion molecule requirements for acute neutrophil emigration in mouse skin. J Immunol 1999;162:5444–8.

[31] Komatsu N, Waki M, Sue M, Tokuda C, Kasaoka T, Nakajima M, et al. Heparanase expression in B16 melanoma cells and peripheral blood neutrophils before and after extravasation detected by novel anti-mouse heparanase monoclonal antibodies. J Immunol Methods 2008;331:82–93.

[32] Gasperini S, Marchi M, Calzetti F, Laudanna C, Vicentini L, Olsen H, et al. Gene expression and production of the monokine induced by IFN-gamma (MIG), IFN-inducible T cell alpha chemoattractant (I-TAC), and IFN-gamma-inducible protein-10 (IP-10) chemokines by human neutrophils. J Immunol 1999;162:4928–37.

[33] Molesworth-Kenyon SJ, Oakes JE, Lausch RN. A novel role for neutrophils as a source of T cell-recruiting chemokines IP-10 and Mig during the DTH response to HSV-1 antigen. J Leukoc Biol 2005;77:552–9.

[34] Seiler P, Aichele P, Bandermann S, Hauser AE, Lu B, Gerard NP, et al. Early granuloma formation after aerosol Mycobacterium tuberculosis infection is regulated by neutrophils via CXCR3-signaling chemokines. Eur J Immunol 2003;33:2676–86.

[35] Wysocki CA, Burkett SB, Panoskaltsis-Mortari A, Kirby SL, Luster AD, McKinnon K, et al. Differential roles for CCR5 expression on donor T cells during graft-versus-host disease based on pretransplant conditioning. J Immunol 2004;173:845–54.